Omniphobic nanofiberous membrane with Pine-needle-like hierarchical nanostructures: Towards enhanced performance for membrane distillation

Xianhui Li,[†,▽] *Weihua Qing,*[†,▽] *Yifan Wu,*[‡] *Senlin Shao,*[†,∥] *Lu Elfa Peng,*[†] *Yang Yang,*[⊥] *Peng Wang,*[§] *Fu Liu,*[#] *Chuyang Y. Tang*[*,†]

[†] Department of Civil Engineering, The University of Hong Kong, Pokfulam, Hong Kong 999077, P. R. China

[‡] Department of Chemistry, The University of Hong Kong, Pokfulam, Hong Kong 999077, P. R. China

[∥] School of Civil Engineering, Wuhan University, Wuhan 430072, P. R. China

[⊥] Department of Chemical Engineering, Imperial College London, London SW7 2AZ, UK

[§]Department of Civil and Environmental Engineering, The Hong Kong Polytechnic University, Hung Hom, Kowloon, Hong Kong 999077, P. R. China

[#] Key Laboratory of Marine Materials and Related Technologies, Ningbo Institute of Materials Technology and Engineering, Chinese Academy of Sciences, Ningbo 315201, P. R. China

Corresponding Author

*Chuyang Y. Tang. E-mail: tangc@hku.hk

[▽] These authors contributed equally to this work.

ABSTRACT: Wetting and fouling phenomena are main concerns for membrane distillation (MD) in treating high salinity industrial wastewater. This work developed an omniphobic membrane by growing titanium dioxide (TiO_2) nanorods on polyvinylidene fluoride-co-hexafluoropropylene (PVDF-HFP) nanofibers using a hydrothermal technique. The TiO_2 nanorods form a uniform pine-needle-like hierarchical nanostructure on PVDF-HFP fibers. A further fluorination treatment provides the membrane with a low-surface-energy omniphobic surface, displaying contact angles of 168° and 153° for water and mineral oil, respectively. Direct contact MD experiments demonstrated that the resulting membrane shows a high and stable salt rejection of >99.9%, while the pristine PVDF-HFP nanofiberous membrane suffers a rejection decline caused by intense pore wetting and oil fouling in the desalination process in presence of surfactant and mineral oil. The superior anti-wetting and anti-fouling behaviors were ascribed to a non-wetting Cassie-Baxter state established by the accumulating of a great deal of air in the hydrophobized hierarchical re-entrant structures. The development of omniphobic membranes with pine-needle-like hierarchical nanostructures provides an approach to mitigate membrane wetting and fouling in the MD process for the water reclamation from industrial wastewater.

KEYWORDS: *Membrane distillation, omniphobic membrane, titanium dioxide nanorods, electrospun nanofibers, antiwetting and antifouling*

■ INTRODUCTION

Membrane distillation (MD) is a thermally driven membrane-based process that utilises a hydrophobic porous membrane to inhibit liquid transport but allow vapor to pass across the membrane.[1,2] MD can operate at relatively low temperatures and thus can use low-grade waste heat to achieve more energy savings.[3] MD membranes are typically fabricated by hydrophobic polymers, including polytetrafluoroethylene[4], polyvinylidene fluoride[5], and polyethylene[6], etc. Nevertheless, challenges of membrane wetting by low surface tension pollutants (e.g. surfactant) and fouling (e.g. by oil) hinder their commercialization.[7-9] To address these challenges, it is desirable to develop a unique omniphobic surface that can repel both water and oil.[10-12]

One effective way to realize omniphobic surfaces is to create a three dimensional (3D) micro/nanoscale re-entrant structure, which can be coupled with a further chemical treatment to lower the surface energy.[13,14] The electrospun nanofibers are attractive substrates for developing omniphobic membranes, because their cylindrical shape is a typical re-entrant structure and is can be further modified to establish hierarchical re-entrant structures.[15] Recently, the unique hierarchical re-entrant structures have been established by depositing nanoparticles such as titanium dioxide (TiO_2) and silicon dioxide (SiO_2) [16,17] onto the nanofiber surface using a wide range of modification approaches, including chemical vapour deposition[18], layer-by-layer[19], and electrospraying technology[20]. Compared to nanoparticles, according to the Wenzel and Cassie-Baxter models, the nanorods architecture can potentially capture more air to restrain the water/oil droplets from touching the membrane surface, resulting in improved liquid-repelling property.[21-23] TiO_2 is a good candidate to fabricate nanorods array because of

its various nanostructures and outstanding properties for extensive applications in photocatalysis[24], solar cells[25], and gas sensors and biosensors[26]. Several studies have reported the fabrication of 3D omniphobic porous materials by depositing TiO_2 nanorods array on inorganic fiberous substrates (carbon fibers, glass fibers, TiO_2 fibers, etc.)[27-30]. However, these materials have not yet been reported for MD applications, since the fragile inorganic substrates can adversely impact their long-term stability and module assembly. Herein, we propose to utilize polymeric nanofibers as substrates to enhance the mechanical stability of such materials.

This study aims to fabricate an omniphobic membrane by the growth of 3D pine-needle-like hierarchical nanostructures on flexible polymetric nanofibers and to elucidate the nanostructure-performance relationship of MD membrane for water reclamation from low surface-tension and oil-containing saline water. A highly thermal stable polyvinylidene fluoride-co-hexafluoropropylene (PVDF-HFP) nanofibrous substrate was prepared by electrospinning to provide high porosity and well interconnected structure.[31] We used a polydopamine (PDA)-based surface modification to decorate the highly non-reactive PVDF-HFP nanofibers in order to induce nucleation of TiO_2 seeds[32,33] before the growth of the 3D pine-needle-like hierarchical nanostructure in a subsequent hydrothermal treatment. To the best of our knowledge, this is the first report on the realization of the growth of nanorods on flexible polymeric nanofibers for applications in MD.

■ MATERIALS AND METHODS

Materials. Poly(vinylidene fluoride-co-hexafluoropropylene) (PVDF-HFP, M_w=455,000), N,N-Dimethylformamide (DMF), dopamine hydrochloride and Tris (hydroxymethyl) aminomethane (Tris-HCl, ≥ 99.0 %) were purchased from Sigma-Aldrich Co., Ltd.

Hydrochloric acid (HCl, 37 wt%), tetrabytyl titanate (98% $Ti(n\text{-}OBu)_4$), and trichloro (1H,1H,2H,2H-tridecafluoro-*n*-octyl) silane (FOTS, 97%) were purchased from Tokyo Chemical Industry Co., Ltd. All other chemicals including acetic acid, absolute ethanol, sodium chloride (NaCl, anhydrous), mineral oil, Tween-80, and sodium dodecyl sulfate (SDS, 99%) were supplied by Dieckman company. Milli-Q water was used in the experiment.

Preparation of the PVDF-HFP/TiO_2-NRs-FOTS nanofibrous membranes. As schematically illustrated in Figure 1, the PVDF-HFP nanofibers were prepared *via* electrospinning using a 20 wt% PVDF-HFP dope solution (dissolved in DMF) under a working voltage of 20 kV (+17.0 kV for spinning jet and −3.0 kV for receiver) at a dope flow rate of 0.8 mL h^{-1}, and a receiving distance of 15 cm.[5] To enhance the adhesion between hydrophilic TiO_2 and highly-non-reactive fluoropolymer PVDF-HFP and to induce crystallization of TiO_2, we coated a PDA layer on the PVDF-HFP surface[32] by immersing the fiber into a 10 mM L^{-1} of Tris-HCl buffer solution with 2 mg mL^{-1} of dopamine (DA) at a pH value of 8.5 for 6 h. The coated PVDF-HFP fibers were thoroughly rinsed using Milli-Q water to move any labile polydopamine.

TiO_2 nanorods were deposited on PDA-coated PVDF-HFP fibers through a two-step hydrothermal procedure for fastening TiO_2 seeds and subsequently growing TiO_2 nanorods. Firstly, a TiO_2 sol-gel solution was synthesized using 1 vol% $Ti(n\text{-}OBu)_4$ as precursors in a mixture solution of deionized water, acetic acid and ethanol (v/v/v, 1:50:150) for 60 min. Both the prepared sol-gel solution and the PDA-coated PVDF-HFP nanofibers were loaded into a Teflon-lined autoclave for hydrothermal reaction at low temperature of 110 °C for 4 h to obtain the TiO_2 seeds fastened PVDF-HFP nanofibers. Afterwards, the fibers were thoroughly rinsed

with Milli-Q water, before being dried in the oven at 60 °C. Subsequently, these seeded nanofibers were subjected to a second hydrothermal treatment using a mixture solution of Ti(n-OBu)$_4$, deionized water and HCl with a volume ratio of 1/30/30 at 110 °C for 12 h to achieve the growth of TiO_2 nanorods on the PVDF-HFP nanofibers (labeled as PVDF-HFP/TiO_2-NRs). The fibers were rinsed with sufficient amount of Milli-Q water to remove any residuals, and then dried in the oven at 60 °C overnight. The as-fabricated PVDF-HFP/TiO_2-NRs nanofibrous membranes were fluorinated using FOTS, which could be immobilized on the TiO_2 surface via covalent bonding.[16,19] A piece of the PVDF-HFP/TiO_2-NRs membrane was treated by evaporating 100 μL FOTS for 30 min in a vacuum oven at 100 °C and 100 kPa. The obtained FOTS-coated PVDF-HFP/TiO_2-NRs nanofiberous membranes were denoted as PVDF-HFP/TiO_2-NRs-FOTS.

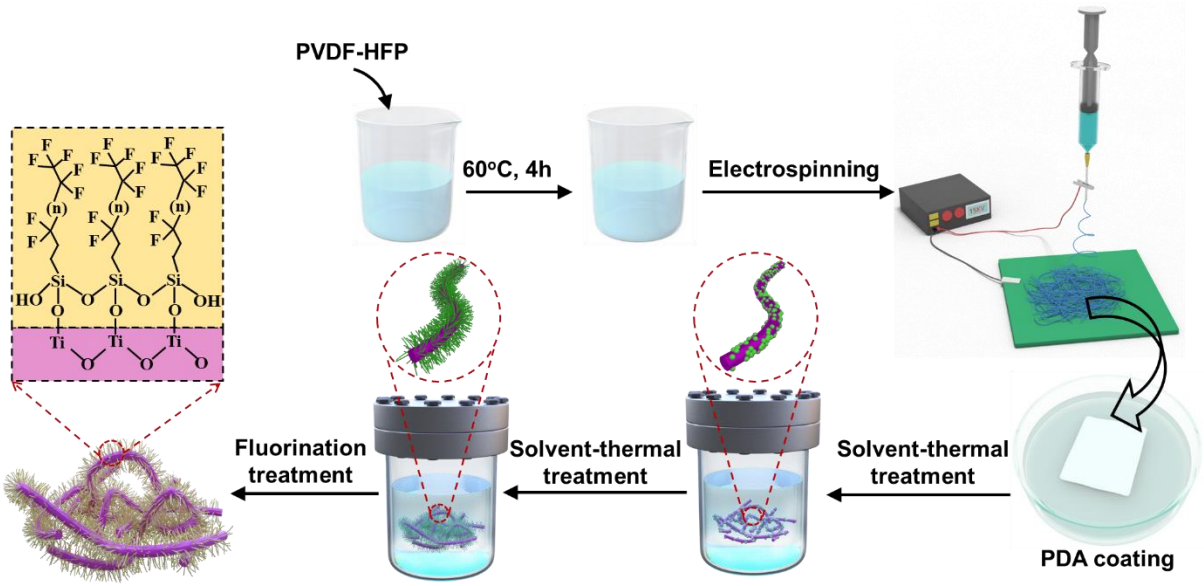

Figure 1. Schematic diagram of the fabrication procedures of the TiO_2-nanorods FOTS modified PVDF-HFP nanofibers.

Membrane Characterization. A Field Emission Gun Scanning Electron Microscope

(SEM, LEO-1530) fitted with an X-ray detector for energy-dispersive X-ray Spectroscopy (EDS, Oxford Instruments X-Max 50) was employed to record the surface morphologies and compositions of membrane. Their functional groups were analyzed by X-ray Photoelectron Spectroscopy (XPS, Thermo Fisher) and Attenuated total reflectance-Fourier transform infrared spectroscopy (ATR-FTIR, Perkin-Elmer). Surface wettability of membrane was studied by contact angle measurements using Kruss DSA 100 (Kruss GmbH, Germany). A Digital Caliper was used to measure the thickness of membrane at five different locations for each sample. The liquid entry pressure (LEP) against water and pore size of membrane were measured by a capillary flow porometer (POROLUX^{TM} 1000, Germany).

In addition, the porosity (ε) of the prepared membrane was measured with the dry mass (M_d) and wet mass (M_w) of membrane samples. The wet membrane was prepared by immersing into isopropyl alcohol for 12 h. The porosity of membrane is calculated as follows:

$$\varepsilon = \frac{(M_w - M_d)/\rho_w}{\left(\frac{M_w - M_d}{\rho_w}\right) - \left(\frac{M_d}{\rho_p}\right)} \times 100\% \quad (1)$$

where ρ_p and ρ_w are polymer density (ρ_p = 17. 7 × 10^5 g/m^3 for PVDF-HFP) and wetting solvent density (ρ_w = 7.68 × 10^5 g/m^3 for isopropyl alcohol), respectively.

Surface Energy Characterization. The surface energy of materials could be calculated by the Owens-Wendt model[34] using the intrinsic contact angles measured on relatively smooth and dense surfaces.[35,36] To obtain the intrinsic contact angle, a simple film casting approach was applied to prepare the flat PVDF-HFP film. The 20 wt% PVDF-HFP dope solution was casted by an automatic film applicator (Elcometer 4340, Elcometer), then it was put in a vacuum oven at 50 °C and 100 kPa to form the PVDF-HFP film. The PVDF-HFP film was modified with TiO_2 nanorods and then subsequently coated by FOTS as described in the previous section.

The contact angles of the PVDF-HFP film and the FOTS-coated nanorods-fastened PVDF-HFP film were determined to be the intrinsic contact angles. The surface energy of the sample is calculated as follows:

$$\frac{\sigma_L(1+\cos(\theta))}{2} = \sqrt{\sigma_L^d}\sqrt{\sigma_S^d} + \sqrt{\sigma_L^p}\sqrt{\sigma_S^p} \quad (2)$$

where σ_S is the surface energy of the film, which originates from dispersive bonding force (σ_S^d) and polar bonding force (σ_S^p). Similarly, σ_L is the surface tension of liquids. σ_L^p and σ_L^d are the polar and dispersive bonding forces of liquids, respectively. θ is the intrinsic contact angle. Water and ethylene glycol were selected as liquids in this study and the corresponding surface tensions were presented in Table S1.

The wetting and fouling behaviors were tested by using a home-made direct contact membrane distillation (DCMD) unit in a counter-current crossflow mode (Figure 2). The membrane coupon has dimensions of length of 6 cm and width of 1.5 cm. The feed solution with 3.5 wt% NaCl was circulated at a crossflow rate of 0.4 L min^{-1}. The feed and permeate temperatures were maintained at 60°C and 20°C, respectively, using two circulator baths (CNSHP, China). The conductivity and weight of the permeate solution were measured by a conductivity meter (SIN-TDS310, Sinomeasure, China) and a digital balance (Adventurer Pro AV8101, OHAUS, USA), respectively. All data were recorded by a computer with a built-in software. The water flux (J) and salt rejection (R) were calculated by Eqs. (3) and (4), as follows:

$$J = \frac{\Delta m}{A \times \rho \times \Delta t} \quad (3)$$

$$R = \frac{C_f - C_p}{C_f} \times 100\% \quad (4)$$

where A is the membrane effective area (9×10^{-4} m^2), ρ is the water density (1×10^3 kg m^{-3}), Δm (kg) is the mass change of the permeate within a certain period of Δt (h), C_f (mol L^{-1}) and

C_p (mol L^{-1}), determined by conductivity meter, are the concentrations of the feed and permeate, respectively.

To investigate the MD antiwetting performance of the pristine and treated PVDF-HFP nanofibrous membranes, SDS was used to decrease the surface tension of the feed solution. In the current study, the SDS concentration was ramped up sequentially (0.1, 0.2, 0.3, 0.4 and 0.5 mM, with each step lasting for one hour).

To further investigate the MD antifouling performance of the pristine and treated PVDF-HFP nanofibrous membranes, a mixed emulsion of mineral oil and Tween-80 was injected in the feed solution. The oil concentration in the feed solution reached to 80, 160, 240, 320, 400 and 480 mg L^{-1} after sequential steps at one-hour interval.

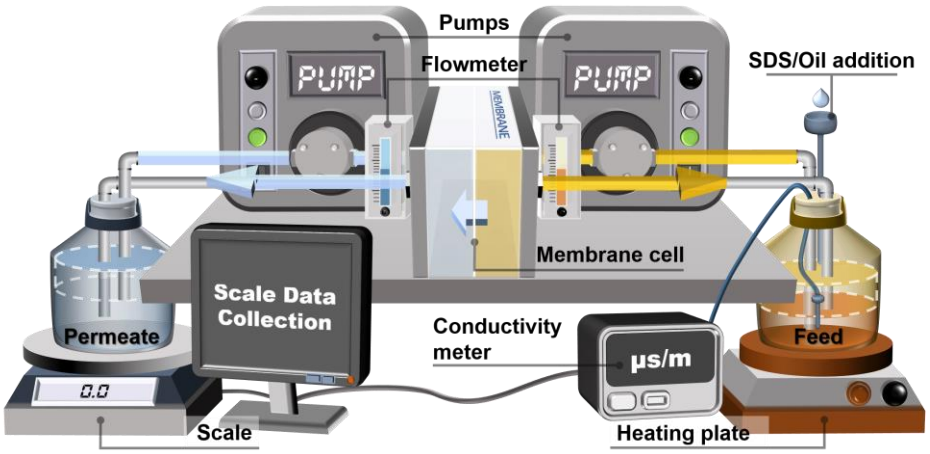

Figure 2. Schematic illustration of direct contact membrane distillation setup.

■ RESULTS AND DISCUSSION

Morphology and structure of the PVDF-HFP/TiO_2-NRs-FOTS nanofibrous membranes. The surface morphologies of the PVDF-HFP nanofibers after each modification step are presented in Figure 3. The electrospun PVDF-HFP nanofibers have an average diameter of 200-400 nm (Figure 3a,b). These nanofibers are interconnected with each other

and form a high-surface-area substrate.[37] The PDA treated PVDF-HFP nanofibers (Figure 3c,d) showed a relatively coarse surface. EDS element mapping shows the presence of nitrogen element on the coated PVDF-HFP substrate (Figure S1), confirming the successful coating of PDA on the PVDF-HFP nanofibers. This PDA coating provides –OH functional groups as anchors for TiO_2 seeds to grow on the non-reactive substrate.[38] After that, a hydrothermal process was utilized for *in situ* growth of nano-sized TiO_2 seeds on the surface of PVDF-HFP nanofibers (Figure 3e,f). Eventually, a dense layer of TiO_2 nanorods with 700-800 nm in length and 50-60 nm in diameter was evenly grown on the PVDF-HFP nanofibers (PVDF-HFP/TiO_2-NRs) to form a hierarchical structure (Figure 3g,h). The titanium and oxygen elements distribution on the surface of nanorods displayed in EDS spectra (Figure S2) confirmed that the features of hierarchical structure were related to the formation of TiO_2 nanorods. The subsequent fluorinated hydrophobization treatment also had almost no obvious effect on the morphology of the PVDF-HFP/TiO_2-NRs nanofiberous membrane (Figure 3i,j and Figure S3).

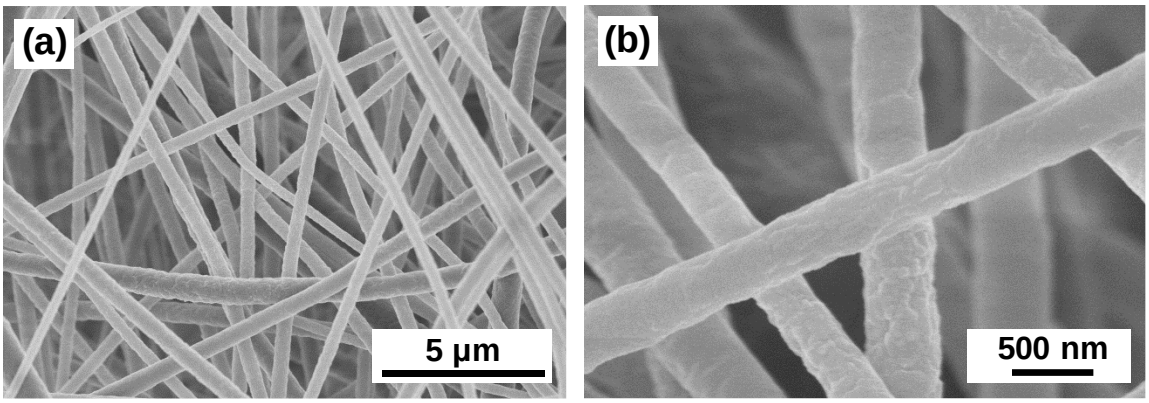

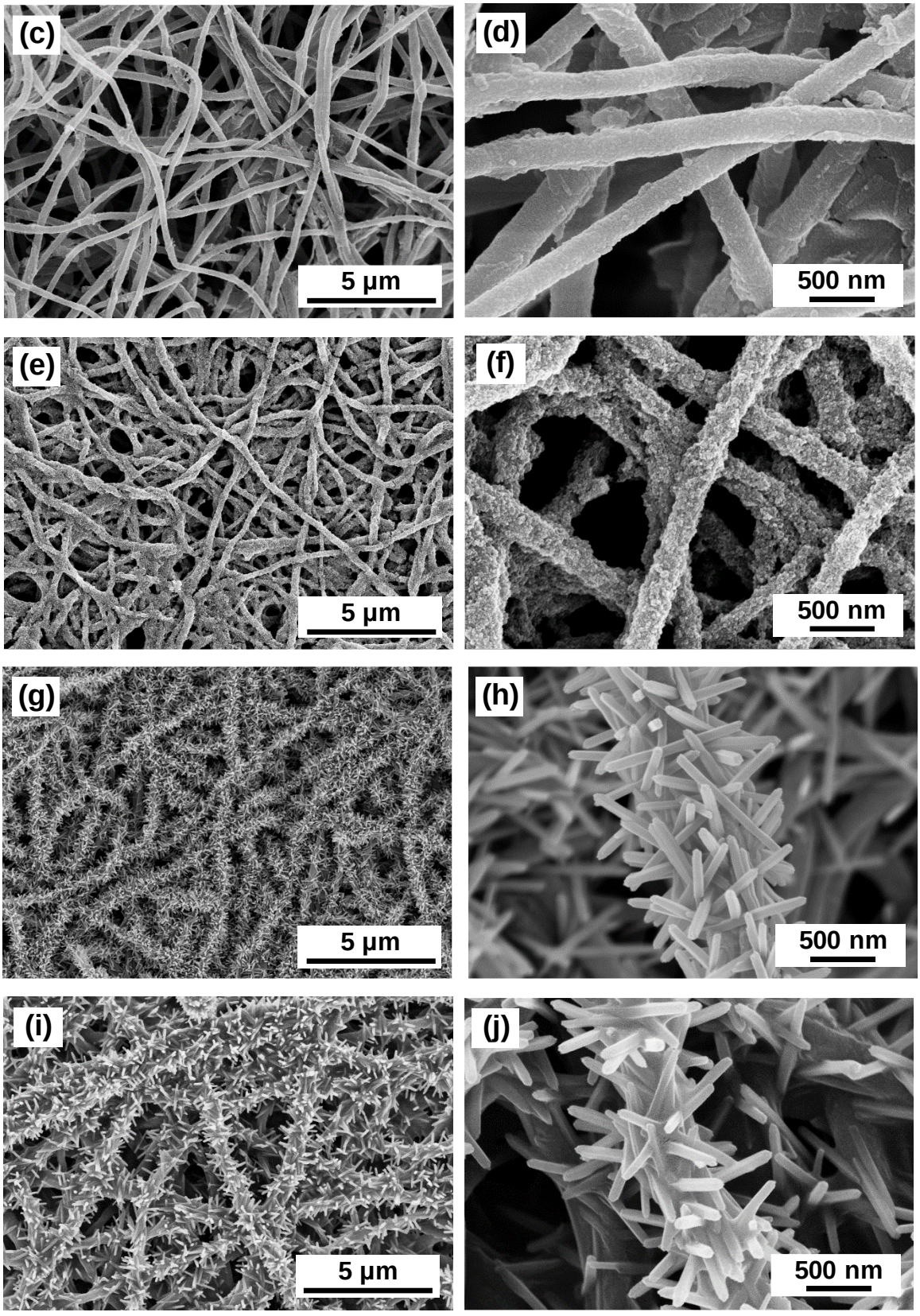

Figure 3. SEM images of (a,b) pristine PVDF-HFP nanofibers, (c,d) PDA coated on PVDF-HFP nanofibers, (e,f) TiO_2 seeds fasten on PVDF-HFP nanofibers, (g,h) PVDF-HFP/TiO_2-NRs

nanofibers, and (i,j) PVDF-HFP/TiO_2-NRs-FOTS nanofibers at different magnifications.

FTIR spectra of pristine PVDF-HFP, PVDF-HFP/TiO_2-NRs, and the FOTS functionalized PVDF-HFP/TiO_2-NRs (Figure 4) confirm the successful modification of the nanofibers. As shown in Figure 4, the peaks of 1402, 874, 840, and 510 cm^{-1} are attributed to the characteristic of $-CH_2-CF_2-$,[39] and the infrared radiation bands found at 1180 and 472 cm^{-1} are considered as the characteristic of PVDF-HFP.[40] Compared to the pristine membrane (Figure 4a), two new absorption features at 460 cm^{-1} and 3400 cm^{-1} appear for the PVDF-HFP/TiO_2-NRs nanofibers (Figure 4b), which are assigned to Ti-O band and hydroxyl group from TiO_2, respectively.[41] Additionally, the peak near 840 cm^{-1} was intensified because it was overlapped with a new vibration peak of Ti–O–Ti band at 820 cm^{-1} from TiO_2.[42] These FTIR results were indicative of the successful immobilization of TiO_2 nanorods on the PVDF-HFP fiber surface. As presented in Figure 4c, two new absorption features at 1014 and 1140 cm^{-1} were abscribed to the stretching vibrations of the Si–O and C–F bonds, respectively, which were formed by the dehydration of the hydroxyls between the hydrolyzed FOTS and the TiO_2 nanorod surface.[43] This suggests a successful fluorination of the PVDF-HFP/TiO_2-NRs surface.

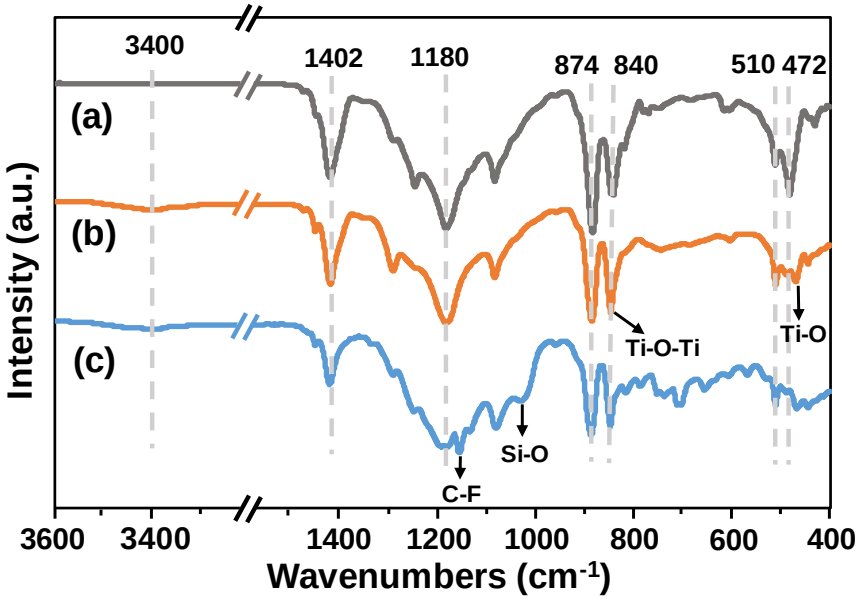

Figure 4. FTIR spectra of (a) pristine PVDF-HFP nanofibers, (b) PVDF-HFP/TiO_2-NRs nanofibers, and (c) PVDF-HFP/TiO_2-NRs-FOTS nanofibers.

The chemical binding between the TiO_2 nanorods and the modified PVDF-HFP membrane surface was further validated by the XPS analysis (Figure 5). In Figure 5a, the XPS survey scan reveals that only three elements (carbon (C), oxygen (O) and fluorine (F)) were observed from the pristine PVDF-HFP nanofibers. In contrast, three new peaks of Ti2p, Si2s and Si2p appear for the modified membrane (Figure 5a and Table 1). The Si2s and Si2p signals resulted from FOTS molecules, indicating the successful fluorinated modification of membrane surface.[42] In addition, the F/C atomic ratio was increased from 1.14 for pristine membrane to 1.52 for TiO_2-NRs-FOTS modified membrane (Table 1), indicating that the FOTS coating introduced a higher fluorine density on the membrane surface and thus greatly reduce the surface free energy. The deposition of FOTS onto TiO_2-NRs surfaces shielded intermediate TiO_2-NRs layer, leading to a lower surface concentration of Ti (0.83% in Table 1). However, it can be clearly seen from the enlarged detail that the peak of Ti2p XPS spectra is constituted by two peaks

with binding energies of 464.4 eV and 458.7 eV (Figure 5b), which corresponds to the Ti $2p_{1/2}$ and Ti $2p_{3/2}$, respectively. It indicates the existence of Ti^{4+} in TiO_2, confirming an effective binding of TiO_2 nanorods onto the PVDF-HFP membranes.[16,44] Additionally, the O1s peak of PVDF-HFP/TiO_2-NRs-FOTS nanofibers was resolved into four peaks (Figure 5c) corresponding to oxygen atoms in the Si-O-Ti (535 eV), Si-O-Si (533.4 eV), Si-OH (531.9 eV), and Si-O (531 eV), respectively.[45] It can be concluded that a dense FOTS network is formed by condensation reactions of the hydrolyzed FOTS molecules through the chemical bonds of Si-O-Si. Furthermore, a strong bonding between TiO_2 nanorods and FOTS layers is formed by the Si-O-Ti covalent bonds due to the condensation reactions between the Si-O alkyl groups of FOTS molecules and the hydroxyl groups of TiO_2-NRs.[46] These results confirm the successful modification of the membrane with TiO_2 nanorods loading and surface fluorination.

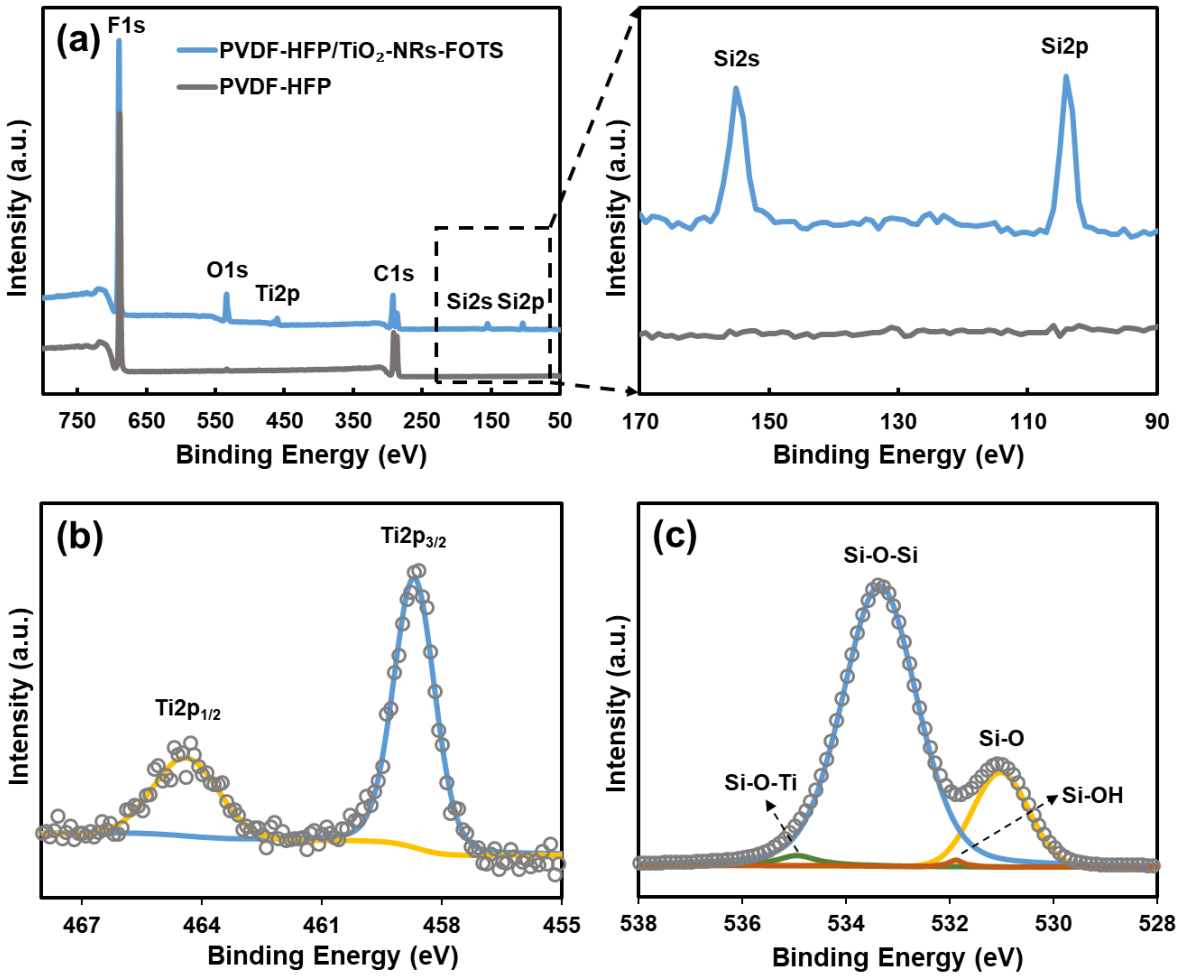

Figure 5. XPS spectra of (a) full survey of pristine PVDF-HFP nanofibers and PVDF-HFP/TiO_2-NRs-FOTS nanofibers, and (b) Ti2p and (c) O1s of PVDF-HFP/TiO_2-NRs-FOTS nanofibers.

Table 1. The surface compositions of the pristine PVDF-HFP nanofibers and PVDF-HFP/TiO_2-NRs-FOTS nanofibers.

	F (at.%)	C (at.%)	Ti (at.%)	O (at.%)	Si (at.%)
PVDF-HFP	52.8 ± 1.8	46.4 ± 1.7	-	0.8 ± 0.1	-
PVDF-HFP/TiO_2-NRs-FOTS	52.1 ± 1.1	34.2 ± 1.9	0.8 ± 0.1	8.3 ± 0.4	4.6 ± 0.3

Wetting resistance of the PVDF-HFP/TiO_2-NRs-FOTS nanofibrous membranes. To assess the membrane wettability, sessile-drop contact angle measurements were carried out with different liquids, including water, glycerol, ethylene glycol and mineral oil with surface

tensions of 72.8, 64, 48 and 30 mN m^{-1}, respectively. As presented in Figure 6a, the PVDF-HFP/TiO_2-NRs-FOTS membrane showed a super-hydrophobicity with a high water contact angle of 168°, whereas the pristine PVDF-HFP membrane displayed a water contact angle of 123°. For the lower surface tension liquids of glycerol and ethylene glycol, the corresponding contact angle for pristine PVDF-HFP membrane was decreased to 110.5 ° and 105 °, respectively. In addition, a rapid wicking occurred when the pristine PVDF-HFP nanofiberous membrane was exposed to mineral oil. In contrast, the PVDF-HFP/TiO_2-NRs-FOTS membrane was not wetted by any of the test liquids and exhibited super-oleophobic property (contact angle > 150°) even with mineral oil. This likely results from their pine-needle-like hierarchical nanostructures, which confine a great deal of air inside its voids and minimize the contact area between the membrane surface and water via the very tips of the spikes (Figure 6b).[47] In addition, PVDF-HFP/TiO_2-NRs-FOTS had significanly lower surface energy (11.2 mN m^{-1}) compared to that of the pristine PVDF-HFP (38.3 mN m^{-1}, Table 2) as a result of the FOTS treatment. Therefore, the enhancement in omniphobic property of the PVDF-HFP/TiO_2-NRs-FOTS nanofibers can be attributed to the decreased liquid/surface interaction and increased liquid/air interaction caused by both the combined low-surface-energy fluorination and the hierarchical texture.[27]

The membrane structural characteristics were also presented in Table 3. Compared to pristine PVDF-HFP membranes, the PVDF-HFP/TiO_2-NRs-FOTS membranes possess lower porosity (75.8%), smaller pore size (0.52 μm) and increased thickness (28 μm), which are attributed to the fiber swelling and shrinkage induced by the hydrothermal treatment and needle-shape rough structures.[48] Liquid entry pressure (LEP), determined as the critical pressure at which

liquid starts to penetrate the membrane pores, is an important factor for preventing of wetting issues.[49] The PVDF-HFP/TiO_2-NRs-FOTS membrane shows a higher LEP (254 kPa) compared to that of the pristine PVDF-HFP membrane (117 kPa) because of its higher contact angle and lower pore size.

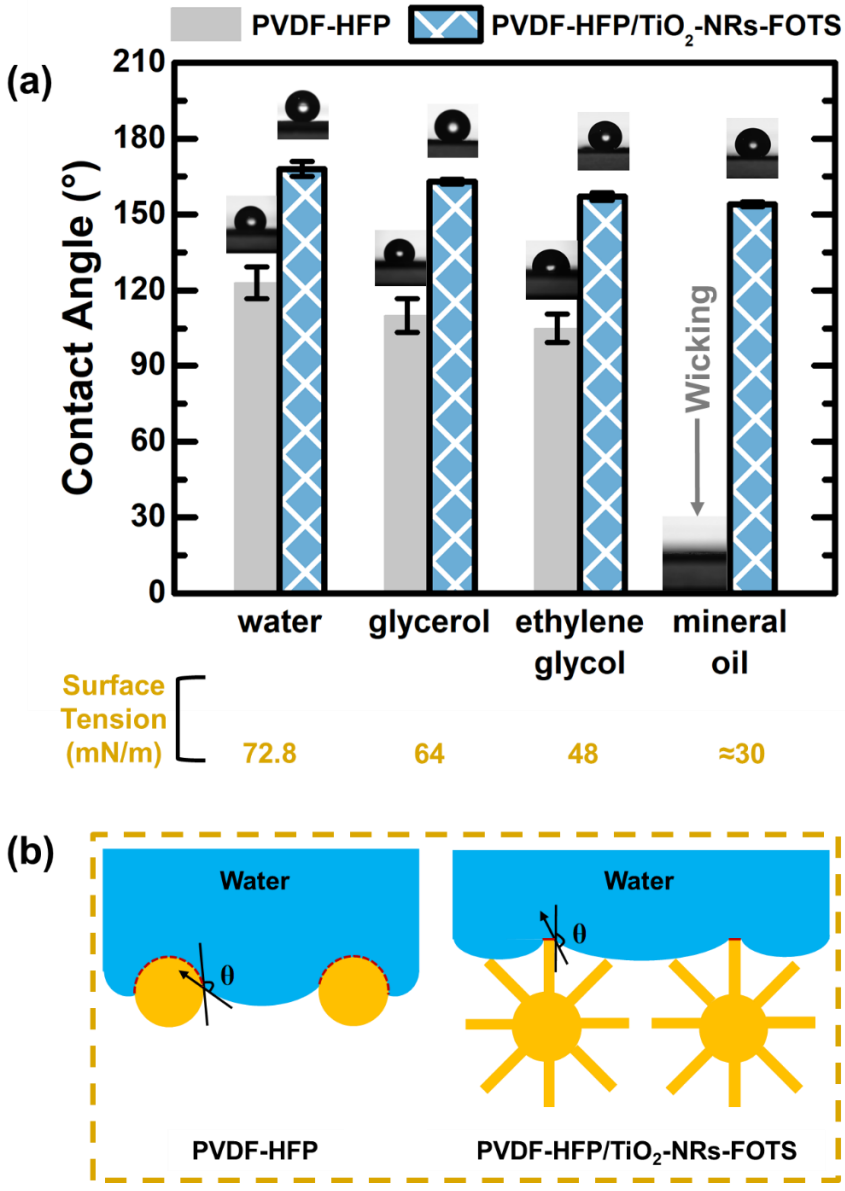

Figure 6. Comparison of (a) contact angles and (b) surface-wetting behaviors between the pristine PVDF-HFP nanofibers and PVDF-HFP/TiO_2-NRs-FOTS nanofibers.

Table 2. Estimation of the surface energies of the pristine PVDF-HFP film and the PVDF-HFP/TiO_2-NRs-FOTS film.

Type of film	Intrinsic contact angle (°)		Surface energy (mN m^{-1})
	Water	Ethylene glycol	
PVDF-HFP	121.3±1.5	89±1.2	38.3±1.4
PVDF-HFP/TiO_2-NRs-FOTS	152.6±1.2	127.3±0.8	11.2±1.2

Table 3. Characteristics of the pristine PVDF-HFP and the PVDF-HFP/TiO_2-NRs-FOTS nanofiberous membranes.

Type of membrane	Thickness (μm)	Porosity (%)	Pore size (μm)	LEP (kPa)
PVDF-HFP	21±2	88.9±1.5	0.85±0.05	117±3
PVDF-HFP/TiO_2-NRs-FOTS	28±3	75.8±0.8	0.52±0.03	254±12

Membrane Performance in DCMD. Despite of the decreased pore size and porosity, the PVDF-HFP/TiO_2-NRs-FOTS membrane showed a water flux of 21.3 L m^{-2} h^{-1}, comparable to 22.6 L m^{-2} h^{-1} of the pristine PVDF-HFP membrane. To access the membrane wetting resistances, the surfactant SDS was injected to the feed solution in steps to decrease the surface tension, thus reducing the LEP and increasing the tendency of membrane wetting. As shown in Figure 7a, when SDS concentration approached 0.1 mM, the water flux of the pristine PVDF-HFP membrane was sharply increased and the salt rejection decreased, indicating the occurrence of severe wetting. In contrast, the PVDF-HFP/TiO_2-NRs-FOTS membrane showed a constant water flux and a nearly complete salt rejection of 99.9% even under the conditions with 0.4 mM SDS. Membrane wetting occurred only as the SDS concentration was increased to 0.5 mM. These results confirmed the greatly enhanced wetting resistance of PVDF-HFP/TiO_2-NRs-FOTS membrane against low surface tension liquids.

To further investigate the antifouling performance, the membranes were tested using saline

mineral oil-in-water emulsion (Figure 7b). When concentration of the oil reached 80 mg/L, the pristine PVDF-HFP membrane showed a sharp reduction of salt rejection and increase of water flux, suggesting a severe wetting and oil fouling on the membrane surface. In comparison, the salt rejection and water flux of the PVDF-HFP/TiO_2-NRs-FOTS membrane were impacted only when the oil concentration was increased to 400 mg/L. This observation demonstrates that modifying membranes with hydrophobic nano/micro scale pine-needle-like structures remarkably enhanced the fouling resistance.[29] Table 4 compares the MD performance and properties of omniphobic nanofiberous membranes developed in previous and current works. Compared to the literature values, the PVDF-HFP/TiO_2-NRs-FOTS membrane in this work shows a comparable flux but an enhanced contact angle, which was primarily attributed to the superhydrophobic property and unique hierarchical structures. The presence of air pockets among the voids of TiO_2 NRs (as shown in Figure 6b) lowers the contact area between water and membrane surface. Because of the synergistic effect of the pine-needle-like hierarchical nanostructures and numerous entrapped air pockets, the membrane has superhydrophobic surfaces with omniphobic characteristics.[23,50] The PVDF-HFP/TiO_2-NRs-FOTS membranes with both effective antifouling and antiwetting behaviors confer a high potential in treatment of challenging industrial wastewaters containing various organic contaminants.

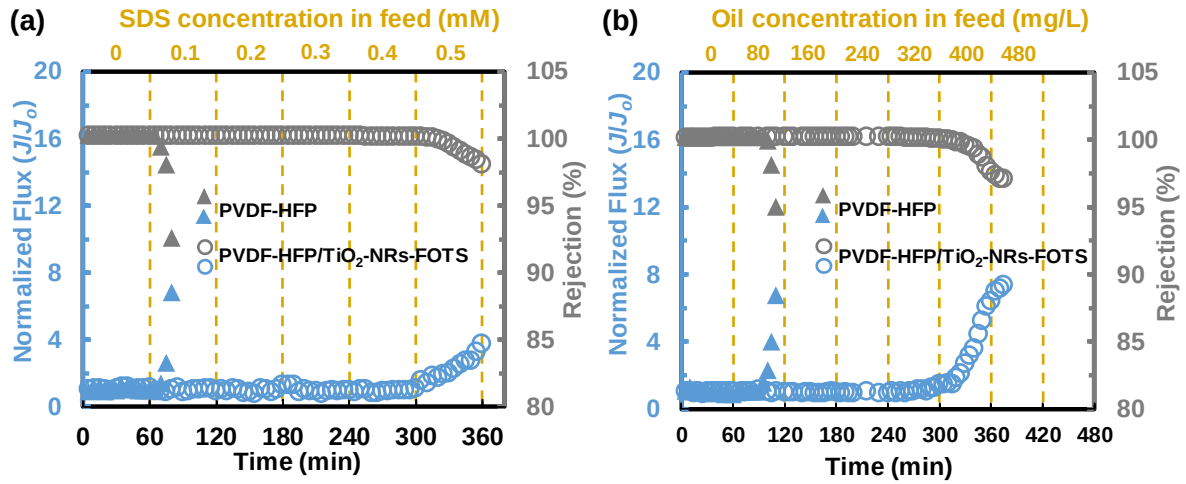

Figure 7. Water flux and salt rejection for the PVDF-HFP/TiO_2-NRs-FOTS nanofiberous membrane and the pristine PVDF-HFP nanofiberous membrane using 35 g/L NaCl saline solution with different (a) SDS concentrations and (b) oil concentrations. For all MD experiments, the temperature of permeate and feed was maintained at 20°C and 60°C, respectively.

Table 4. Comparision of omniphobic nanofiberous membranes for membrane distillation.

Substrate	Modified method	Omniphobicity	MD type	Feed composition	Temperature difference (°C)	Flux (L m^{-2} h^{-1})	Ref.
PVDF nanofiber	CF_4 plasma treatment	WCA 160°; CA 147° for mineral oil	AGMD	RO brine with maxmium 0.7 mM SDS	40	15.2	15
PVDF-HFP nanofiber	Coating fluorined SiNPs followed by hydrophilization	WCA 156°; CA 159° for mineral oil	DCMD	35 g/L NaCl solution with 1000 ppm crude oil	40	~14.1	51
PVDF-HFP nanofiber	Grafting SiNPs on nanofibers followed by fuorination	WCA 150°; CA 135° for mineral oil	DCMD	35 g/L NaCl solution with maxmium 0.3 mM SDS	40	~12.5	31
PVDF nanofiber	Modifying nanofibers with fuorination	WCA 157°; CA 130° for mineral oil	DCMD	35 g/L NaCl solution with maxmium 0.1 mM SDS	40	~25	52
PVDF-HFP nanofiber	One-step electrospinning of fluorinated PVDF-HFP	WCA 154°; CA 148° for mineral oil	DCMD	35 g/L NaCl solution with maxmium 0.3 mM SDS	40	~8	53
Cellulose nanofiber	One-step electrospinning of cellulose acetate and SiNPs followed by fuorination	WCA 155°; CA 120° for castor oil	DCMD	35 g/L NaCl solution with maxmium 0.5 mM SDS	33	13.6	54
Cellulose nanofiber	Depositing SiNPs on nanofibers followed by fuorination	WCA 150°; CA 138° for mineral oil	DCMD	35 g/L NaCl solution with maxmium 0.4 mM SDS	40	46.3	17
PVDF-HFP nanofiber	Growing TiO_2-NRs on nanofibers followed by fuorination	WCA 168°; CA 153° for mineral oil	DCMD	35 g/L NaCl solution with maxmium 0.5 mM SDS, and with maximum 400 ppm mineral oil, respectively	40	21.3	This work

SiNPs: Silica nanoparticles; CA: Contact angle; WCA: Water contact angle; AGMD: Air gap membrane distillation.

■ CONCLUSION

An omniphobic PVDF-HFP nanofiberous membrane with pine-needle-like hierarchical TiO_2-nanorods was fabricated *via* a hydrothermal technique followed by a fluorination treatment. Detailed membrane characterization confirms that TiO_2 nanorods with 700-800 nm in length and 50-60 nm in diameter were tightly bound onto the PVDF-HFP nanofiberous membranes, while the structure of nanofiber substrate remained nearly unchanged after the modification. Growing hierarchical nanorod structures on the PVDF-HFP fibers resulted in large-volume air-trapping pockets. The resulting membrane therefore displayed high contact angles for water (168^o) and mineral oil (153^o). The DCMD experiments demonstrated that the resulting membrane presented enhanced fouling and wetting resistance in comparison with the pristine PVDF-HFP membrane in treating feed solutions containing surfactants and/or mineral oil emulsion. The resulting omniphobic membrane thus has great potential for water reclamation from industrial wastewater.

■ ASSOCIATED CONTENT

Supporting Information

Additional information includes: Surface tension of liquids used; SEM and EDS mapping images of the PDA coated PVDF-HFP, PVDF-HFP/TiO_2-NRs, and PVDF-HFP/TiO_2-NRs-FOTS nanofiberous membranes.

■ AUTHOR INFORMATION

Corresponding Author

* E-mail: tangc@hku.hk (C.Y.T)

ORCID

Xianhui Li: 0000-0001-6500-908X

Weihua Qing: 0000-0002-6624-9509

Yang Yang: 0000-0003-4518-6411

Peng Wang: 0000-0003-0856-0865

Fu Liu: 0000-0003-0041-1873

Chuyang Y. Tang: 0000-0002-7932-6462

Author Contributions

$^{\nabla}$ X.L. and W.Q. contributed equally to this work and considered to be first co-authors.

Notes

The authors declare no competing financial interest.

■ ACKNOWLEDGMENTS

The study is supported by the Joint Research Scheme (National Natural Science Foundation of China and Research Grants Council of Hong Kong) (N_HKU706/16). We also appreciate the Seed Funding for Strategic Interdisciplinary Research Scheme, the University of Hong Kong and the State Key Laboratory of Separation Membranes and Membrane Processes (Tianjin Polytechnic University) (No. M3-201701).

■ REFERENCES

(1) Alkhudhiri, A.; Darwish, N.; Hilal, N. Membrane distillation: A comprehensive review. *Desalination* **2012**, *287*, 2-18.

(2) Dong, Z. Q.; Wang, B. J.; Ma, X. H.; Wei, Y. M.; Xu, Z. L. FAS grafted electrospun poly(vinyl alcohol) nanofiber membranes with robust superhydrophobicity for membrane distillation. *ACS Appl. Mater. Interfaces* **2015**, *7*, 22652-22659.

(3) Dow, N.; Gray, S.; Li, J. D.; Zhang, J. H.; Ostarcevic, E.; Liubinas, A.; Atherton, P.; Roeszler, G.; Gibbs, A.; Duke, M. Pilot trial of membrane distillation driven by low grade waste heat: Membrane fouling and energy assessment. *Desalination* **2016**, *391*, 30-42.

(4) Qing, W. H.; Shi, X. N.; Deng, Y. J.; Zhang, W. D.; Wang, J. Q.; Tang, C. Y. Robust superhydrophobic-superoleophilic polytetrafluoroethylene nanofibrous membrane for oil/water separation. *J. Membr. Sci.* **2017**, *540*, 354-361.

(5) Qing, W. H.; Wang, J. Q.; Ma, X. H.; Yao, Z. K.; Feng, Y.; Shi, X. N.; Liu, F.; Wang, P.; Tang, C. Y. One-Step tailoring surface roughness and surface chemistry to prepare superhydrophobic polyvinylidene fluoride (PVDF) membranes for enhanced membrane distillation performances. *J. Colloid. Interf. Sci.* **2019**, *553*, 99-107.

(6) Zuo, J.; Bonyadi, S.; Chung, T. S. Exploring the potential of commercial polyethylene membranes for desalination by membrane distillation. *J. Membr. Sci.* **2016**, *497*, 239-247.

(7) Chang, J.; Shi, Y.; Wu, M.; Li, R.; Shi, L.; Jin, Y.; Qing, W. H.; Tang, C. Y.; Wang, P. Solar-assisted fast cleanup of heavy oil spills using photothermal sponge. *J. Mater. Chem.*

A **2018**, 6, 9192-9199.

(8) Li, C.; Li, X.; Du, X.; Tong, T.; Cath, T. Y.; Lee, J. Antiwetting and antifouling Janus membrane for desalination of saline oily wastewater by membrane distillation. *ACS Appl. Mater. Interfaces* **2019**, *11*, 18456-18465.

(9) Shao, S.; Wang, Y.; Shi, D.; Zhang, X.; Tang, C. Y.; Liu, Z.; Li, J. Biofouling in ultrafiltration process for drinking water treatment and its control by chlorinated-water and pure water backwashing. *Sci. Total Environ.* **2018**, *644*, 306-314.

(10) Lin, S. H.; Nejati, S.; Boo, C.; Hu, Y. X.; Osuji, C. O.; Elimelech, M. Omniphobic membrane for robust membrane distillation. *Environ. Sci. Technol. Lett.* **2014**, *1*(11), 443-447.

(11) Wang, W.; Du, X.; Vahabi, H.; Zhao, S.; Yin, Y.; Kota, A. K.; Tong, T. Trade-off in membrane distillation with monolithic omniphobic membranes. *Nat. Commun.* **2019**, *10*, 3220.

(12) Liu, T. L.; Kim, C. J. C. Turning a surface super-repellent even to completely wetting liquids. *Science* **2014**, *346*, 1096.

(13) Hammami, M. A.; Croissant, J. G.; Francis, L.; Alsaiari, S. K.; Anjum, D. H.; Ghaffour, N.; Khashab, N. M. Engineering hydrophobic organosilica nanoparticle-doped nanofibers for enhanced and fouling resistant membrane distillation. *ACS Appl. Mater. Interfaces* **2017**, *9*, 1737-1745.

(14) Wong, T. S.; Kang, S. H.; Tang, S. K. Y.; Smythe, E. J.; Hatton, B. D.; Grinthal, A.; Aizenberg, J. Bioinspired self-repairing slippery surfaces with pressure-stable omniphobicity. *Nature* **2011**, *477*, 443.

(15) Woo, Y. C.; Chen, Y.; Tijing, L. D.; Phuntsho, S.; He, T.; Choi, J. S.; Kim, S. H.; Shon, H. K. CF_4 plasma-modified omniphobic electrospun nanofiber membrane for produced water brine treatment by membrane distillation. *J. Membr. Sci.* **2017**, *529*, 234-242.

(16) Qin, A.; Li, X.; Zhao, X.; Liu, D.; He, C. Engineering a highly hydrophilic PVDF membrane via binding TiO_2 nanoparticles and a PVA layer onto a membrane surface. *ACS Appl. Mater. Interfaces* **2015**, *7*, 8427-8436.

(17) Dizge, N.; Shaulsky, E.; Karanikola, V. Electrospun cellulose nanofibers for superhydrophobic and oleophobic membranes. *J. Membr. Sci.* **2019**, *590*, 117271.

(18) Guo, F.; Servi, A.; Liu, A.; Gleason, K. K.; Rutledge, G. C. Desalination by membrane distillation using electrospun polyamide fiber membranes with surface fluorination by chemical vapor deposition. *ACS Appl. Mater. Interfaces* **2015**, *7*, 8225-8232.

(19) Woo, Y. C.; Kim, Y.; Yao, M.; Tijing, L. D.; Choi, J. S.; Lee, S.; Kim, S. H.; Shon, H. K. Hierarchical composite membranes with robust omniphobic surface using layer-by-layer assembly technique. *Environ. Sci. Technol.* **2018**, *52*, 2186-2196.

(20) Deka, B. J.; Lee, E. J.; Guo, J.; Kharraz, J.; An, A. K. Electrospun nanofiber membranes incorporating PDMS-Aerogel superhydrophobic coating with enhanced flux and improved antiwettability in membrane distillation. *Environ. Sci. Technol.* **2019**, *53*(9), 4948-4958.

(21) Bok, H. M.; Kim, S.; Yoo, S. H.; Kim, S. K.; Park, S. Synthesis of perpendicular nanorod arrays with hierarchical architecture and water slipping superhydrophobic

properties. *Langmuir* **2008**, *24*, 4168-4173.

(22) Tuteja, A.; Choi, W.; Ma, M.; Mabry, J. M.; Mazzella, S. A.; Rutledge, G. C.; McKinley, G. H.; Cohen, R. E. Designing superoleophobic surfaces. *Science* **2007**, *318*, 1618.

(23) Wang, M. X.; Liu, G. C.; Yu, H.; Lee, S. H.; Wang, L.; Zheng, J. Z.; Wang, T.; Yun, Y. B.; Lee, J. K. ZnO nanorod array modified PVDF membrane with superhydrophobic surface for vacuum membrane distillation application, *ACS Appl. Mater. Interfaces* **2018**, *10*, 13452-13461.

(24) Cho, I. S.; Chen, Z.; Forman, A. J.; Kim, D. R.; Rao, P. M.; Jaramillo, T. F.; Zhen, X. Branched TiO_2 nanorods for photoelectrochemical hydrogen production. *Nano Lett.* **2011**, *11*, 4978-4984.

(25) Liu, B.; Aydil, E. S. Growth of oriented single-crystalline rutile TiO_2 nanorods on transparent conducting substrates for dye-sensitized solar cells. *J. Am. Chem. Soc.* **2009**, *131*, 3985-3990.

(26) Tian, J.; Zhao, Z.; Kumar, A.; Boughton, R. I.; Liu, H. Recent progress in design, synthesis, and applications of one-dimensional TiO_2 nanostructured surface heterostructures: a review. *Chem. Soc. Rev.* **2014**, *43*, 6920-6937.

(27) Yuan, D.; Zhang, T.; Guo, Q.; Qiu, F.; Yang, D.; Ou, Z. Superhydrophobic hierarchical biomass carbon aerogel assembled with TiO_2 nanorods for selective immiscible oil/water mixture and emulsion separation. *Ind. Eng. Chem. Res.* **2018**, 57(43), 14758-14766.

(28) Liu, W.; Zhang, L.; Cao, L. X.; Su, G.; Wang, Y. G. Glass fibers templated

preparation of TiO_2 microtubes assembled from nano/micro hierarchical TiO_2 crystals. *J. Alloy. Compd.* **2011**, 509, 3419-3424.

(29) Zhang, Y. Y.; Chen, Y.; Hou, L. L.; Guo, F. Y.; Liu, J. C.; Qiu, S. S.; Xu, Y.; Wang, N.; Zhao, Y. Pine-branch-like TiO_2 nanofibrous membrane for high efficiency strong corrosive emulsion separation. *J. Mater. Chem. A* **2017**, *5*(31), 16134-16138.

(30) Guo, H.; Fuchs, P.; Casdorff, K.; Michen, B.; Chanana, M.; Hagendorfer, H.; Romanyuk, Y. E.; Burgert, I. Bio-inspired superhydrophobic and omniphobic wood surfaces. *Adv. Mater. Interfaces* **2017**, *4*, 1600289.

(31) Lee, J.; Boo, C.; Ryu, W. H.; Taylor, A. D.; Elimelech, M. Development of omniphobic desalination membranes using a charged electrospun nanofiber scaffold. *ACS Appl. Mater. Interfaces* **2016**, *8*, 11154-11161.

(32) Cui, J.; Ma, C.; Li, Z.; Wu, L.; Wei, W.; Chen, M.; Peng, B.; Deng Z. Polydopamine-functionalized polymer particles as templates for mineralization of hydroxyapatite: Biomimetic and in vitro bioactivity. *RSC Adv.* **2016**, *6*, 6747-6755.

(33) Ho, C. C.; Ding, S. J. Dopamine-induced silica/polydopamine hybrids with controllable morphology. *Chem. Commun.* **2014**, *50*, 3602-3605.

(34) Owens, D. K.; Wendt, R. C. Estimation of the surface free energy of polymers. *J. Appl. Polym. Sci.* **1969**, *13*(8), 1741-1747.

(35) Nishino, T.; Meguro, M.; Nakamae, K.; Matsushita, M.; Ueda, Y. The lowest surface free energy based on $-CF_3$ alignment, *Langmuir* **1999**, *15*(13), 4321-4323.

(36) Boo, C.; Lee, J.; Elimelech, M. Engineering surface energy and nanostructure of microporous films for expanded membrane distillation applications. *Environ. Sci.*

Technol. **2016**, *50*, 8112-8119.

(37) Si, Y.; Fu, Q.; Wang, X.; Zhu, J.; Yu, J.; Sun, G.; Ding, B. Superelastic and superhydrophobic nanofiber-assembled cellular aerogels for effective separation of oil/water emulsions. *ACS Nano **2015**, 9*(4), 3791-3799.

(38) Yan, J.; Yang, L. P.; Lin, M. F.; Ma, J.; Lu, X. H.; Lee, P. S. Polydopamine spheres as active templates for convenient synthesis of various nanostructures. *Small* **2013**, *9*(4), 596-603.

(39) Wongchitphimon, S.; Wang, R.; Jiraratananon, R. Surface modification of polyvinylidene fluoride-co-hexafluoropropylene (PVDF-HFP) hollow fiber membrane for membrane gas absorption. *J. Membr. Sci.* **2011**, *381*, 183-191.

(40) Feng, Y.; Li, W. L.; Hou, Y. F.; Yu, Y.; Cao, W. P.; Zhang, T. D.; Fei, W. D. Enhanced dielectric properties of PVDF-HFP/$BaTiO_3$-nanowire composites induced by interfacial polarization and wire-shape. *J. Mater. Chem. C* **2015**, *3*, 1250-1260.

(41) Shahabadi, S. M. S.; Rabiee, H.; Seyedi, S. M.; Mokhtare, A.; Brant, J. A. Superhydrophobic dual layer functionalized titanium dioxide/polyvinylidene fluoride-co-hexafluoropropylene (TiO_2/PH) nanofibrous membrane for high flux membrane distillation. *J. Membr. Sci.* **2017**, *537*, 140-150.

(42) Ren, L. F.; Xia, F.; Chen, V.; Shao, J.; Chen, R.; He, Y. TiO_2-FTCS modified superhydrophobic PVDF electrospun nanofibrous membrane for desalination by direct contact membrane distillation. *Desalination* **2017**, *423*, 1-11.

(43) Huang, J.; Wang, S.; Lyu, S. Facile preparation of a robust and durable superhydrophobic coating using biodegradable lignin-coated cellulose nanocrystal

particles. *Materials* **2017**, *10*, 1080.

(44) Yang, Y.; Wang, H.; Li, J. X.; He, B. Q.; Wang, T. H.; Liao, S. J. Novel functionalized nano-TiO_2 loading electrocatalytic membrane for oily wastewater treatment. *Environ. Sci. Technol.* **2012**, *46*, 6815-6821.

(45) Yu, X.; Qi, H.; Huang, Z.; Zhang, B.; Liu, S. Preparation and characterization of spherical b-cyclodextrin/urea-formaldehyde microcapsules modified by nano-titanium oxide. *RSC Adv.* **2017**, *7*, 7857-7863.

(46) Meng, S.; Mansouri, J.; Ye, Y.; Chen, V. Effect of templating agents on the properties and membrane distillation performance of TiO_2-coated PVDF membranes. *J. Membr. Sci.* **2014**, *450*, 48-59.

(47) Bahng, J. H.; Yeom, B.; Wang, Y.; Tung, S. O.; Hoff, J. D.; Kotov, N. Anomalous dispersions of 'hedgehog' particles. *Nature* **2015**, *517*, 596-599.

(48) Qing, W. H.; Shi, X. N.; Zhang, W. D.; Wang, J. Q.; Wu, Y. F.; Wang, P.; Tang, C. Y. Solvent-thermal induced roughening: A novel and versatile method to prepare superhydrophobic membranes. *J. Membr. Sci.* **2018**, *564*, 465-472.

(49) Li, X.; Yu, X. F.; Cheng, C.; Deng, L.; Wang, M.; Wang, X. F. Electrospun superhydrophobic organic/inorganic composite nanofibrous membranes for membrane distillation. *ACS Appl. Mater. Interfaces* **2015**, *7*, 21919-21930.

(50) Deka, B. J.; Guo, J.; Khanzada, N. K.; An, A. K. Omniphobic re-entrant PVDF membrane with ZnO nanoparticles composite for desalination of low surface tension oily seawater. *Water Res.* **2019**, *165*, 114982.

(51) Huang, Y. X.; Wang, Z.; Jin, J.; Lin, S. Novel Janus membrane for membrane

distillation with simultaneous fouling and wetting resistance. *Environ. Sci. Technol.* **2017**, *51*, 13304-13310.

(52) Deng, L.; Ye, H.; Li, X.; Li, P.; Zhang, J.; Wang, X.; Zhu, M.; Hsiao, B. S. Self-roughened omniphobic coatings on nanofibrous membrane for membrane distillation. *Sep. Purif. Technol.* **2018**, *206*, 14-25.

(53) Lu, C.; Su, C.; Cao, H.; Ma, X.; Duan, F.; Chang, J.; Li, Y. F-POSS based omniphobic membrane for robust membrane distillation. *Mater. Lett.* **2018**, *228*, 85-88.

(54) Hou, D.; Ding, C.; Fu, C.; Wang, D.; Zhao, C.; Wang, J. Electrospun nanofibrous omniphobic membrane for anti-surfactant-wetting membrane distillation desalination. *Desalination* **2019**, *468*, 114068.

TOC Art

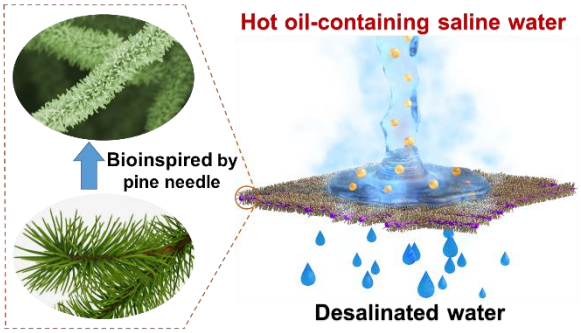
Hot oil-containing saline water
Bioinspired by
pine needle
Desalinated water